Geophysical Research Letters

RESEARCH LETTER
10.1029/2019GL086880

Key Points:
- New multi-mission altimeter products show regional differences in wave height climatologies and trends
- Global Hs trends from latest altimeter wave product appear more positive, though with spatially similar variation
- Uncertainty in means and trends could originate from altimeter wave height calibration and processing choices

Supporting Information:
- Supporting Information S1

Correspondence to:
B. W. Timmermans,
ben.timmermans@gmail.com

Citation:
Timmermans, B. W., Gommenginger, C. P., Dodet, G., & Bidlot, J.-R. (2020). Global wave height trends and variability from new multimission satellite altimeter products, reanalyses, and wave buoys. *Geophysical Research Letters*, *47*, e2019GL086880. https://doi.org/10.1029/2019GL086880

Received 31 DEC 2019
Accepted 26 MAR 2020
Accepted article online 9 APR 2020

Global Wave Height Trends and Variability from New Multimission Satellite Altimeter Products, Reanalyses, and Wave Buoys

B. W. Timmermans[1], C. P. Gommenginger[1], G. Dodet[2], and J.-R. Bidlot[3]

[1]National Oceanography Centre, European Way, Southampton, UK, [2]Laboratoire d'Océanographie Physique et Spatiale (LOPS), CNRS, IRD, Ifremer, IUEM, Université de Bretagne Occidentale, Brest, France, [3]European Centre for Medium-range Weather Forecasts, Reading, UK

Abstract Long-term changes in ocean surface waves are relevant to society and climate research. Significant wave height climatologies and trends over 1992–2017 are intercompared in four recent high-quality global datasets using a consistent methodology. For two products based on satellite altimetry, including one from the European Space Agency Climate Change Initiative for Sea State, regional differences in mean climatology are linked to low and high sea states. Trends from the altimetry products, and two reanalysis and hindcast datasets, show general similarity in spatial variation and magnitude but with major differences in equatorial regions and the Indian Ocean. Discrepancies between altimetry products likely arise from differences in calibration and quality control. However, multidecadal observations at two buoy stations also highlight issues with wave buoy data, raising questions about their unqualified use, and more fundamentally about uncertainty in all products.

Plain Language Summary Changes to ocean waves over decades and longer are of considerable importance to the climate, the society, and the marine economy. Accurate observations of waves spanning many decades are required to understand long-term changes, but the challenges and cost of measuring waves worldwide with devices like buoys means that alternatives like Earth-orbiting satellites become attractive. We compare two recently published global wave products derived from the same satellite observations, with two high-quality products from computer simulations and buoy measurements. Using a consistent methodology, we find important differences between the satellite products, and the simulations, in the reported average global wave conditions, and their evolution in time. The disagreement between the satellite products points to complex differences in the way satellite data are corrected, which raises questions about uncertainty in these products, and more generally, about what is our most reliable long-term observational record of sea state.

1. Introduction

Sea state refers to the properties of wind-generated surface waves (Piollé, Dodet & Quilfen, et al., 2020) that may be characterized in many ways, from summary statistics like significant wave height, to complete directional wind-wave spectra. Accurate knowledge of ocean waves and their variability is crucial to numerous ocean and coastal applications, but increasingly also to climate through the mediating role of waves in air-sea interactions, their contributions to global ocean circulation and their multiple impacts through dangerous sea states (Cardone et al., 2015), coastal wave-driven flooding (Storlazzi et al., 2018), coastal erosion (Barnard et al., 2017), and changing sea-ice interactions (Massom et al., 2018; Thomas et al., 2019). Sea state has been studied across many spatial and temporal scales using many types of observations and models, advancing understanding of extreme wave conditions (Alves & Young, 2003; Breivik et al., 2014; Izaguirre et al., 2011; Young et al., 2012), the strong relationships with atmospheric modes of variability (Castelle et al., 2018; Dodet et al., 2010; Woolf et al., 2002), local impacts on circulation patterns and hurricanes (Appendini et al., 2014; Shimura et al., 2015), and long-term trends over the recent era (Semedo et al., 2011; Stopa et al., 2013; Young & Ribal, 2019) and under future climate change scenarios (Bricheno & Wolf, 2018; Camus et al., 2017; Morim et al., 2018, 2019).

Many studies of sea state variability rely on reanalyses and hindcasts that typically use available in situ observations for validation. However, because in situ data are sparse—mostly limited to a few Northern

Hemisphere wave buoys with discontinuous long-term temporal coverage—great reliance is placed upon the ability of the underlying numerical wind and wave simulation systems to reproduce realistic spatiotemporal dependence structures. Camus et al. (2017) highlighted that numerous factors contribute to the variability seen in sea state simulations, beginning with the generation of the wind fields, the downscaling approach and postprocessing, for example, post hoc bias correction. The diversity of source data arising from these factors gives rise to questions of consistency between datasets, absolute accuracy, and available means of independent validation.

Unfortunately, the use of data buoys to study long-term sea state variability is fraught by problems associated with consistency of buoy output and validation methodologies. Aside from the impact of buoy selection, quality control and postprocessing, exploiting wave buoy data for climate studies can be hindered by steps in buoy output linked to poorly documented changes in sensors and hulls, processing upgrades, occasional deployment relocations and prolonged data losses due to operational malfunction and maintenance. While this issue has been recognized by the community, such as the Joint WMO/IOC Technical Commission for Oceanography and Marine Meteorology, Data Buoy Cooperation Panel (Ardhuin et al., 2019; JCOMM DBCP, 2019; Swail et al., 2009), the number of detailed published studies is limited (Gemmrich et al., 2011). The challenge and cost of direct wave measurements with buoys have motivated investigations of other observation methods, for example, with land- or ice-based seismometers (Ardhuin et al., 2011; Bromirski et al., 1999; Hell et al., 2019). While these data offer enormous potential for long-term wave climate research, the lack of maturity and access currently limits their use.

Finally, satellite remote sensing of the ocean offers another readily accessible source of sea state data. Nadir-pointing altimeters provide high-quality measurements of significant wave height and wind speed (Gommenginger et al., 2002; Queffeulou, 2004), while valuable measurements of swell height, period, and direction can be extracted from spaceborne synthetic aperture radar images (Collard et al., 2005; Lehner et al., 2000). Although the long-term consistency and accuracy of multimission satellite data depend on careful calibration and quality control—to address instrument biases and drifts and discrepancies between retrieval algorithms (Ash et al., 2010; ESA, 2019; Queffeulou, 2004; Ribal & Young, 2019; Zieger et al., 2009)—these data are attractive for their global coverage, fine spatial resolution, and regular temporal revisits. For altimetry, the satellite time series now spans over 30 years, starting in 1985 with GEOSAT and presently supported by six concurrent satellites (SARAL AltiKa, CRYOSAT-2, JASON-3, SENTINEL-3A, SENTINEL-3B, and CFOSAT). The growing satellite record motivates new global analyses, including investigations of decadal changes in ocean wave climate. The recent development and release of new high-quality multimission altimeter products of significant wave height (ESA, 2019; Ribal & Young, 2019) make long-term analyses more accessible than ever before.

In this paper, we examine the representation of mean significant wave height (Hs) in four recent Sea State Climate Data Records, including two satellite altimeter products by Ribal and Young (2019) (hereafter RY2019) and the ESA Climate Change Initiative for Sea State (hereafter CCI2019), and two ERA5-based reanalysis and hindcast surface wave products from the European Centre for Medium-Range Weather Forecasts (ECMWF). Details of the four products are summarized in Table S1 in the supporting information. The RY2019 calibrated altimeter dataset underpins the global trends for mean and extreme Hs reported by (Young & Ribal, 2019), which represent the most comprehensive and up-to-date observation-based assessment of global sea state variability to date, and has become the key reference dataset used to validate wave climate projections (Morim et al., 2019). Here, comparisons focus primarily on global climatologies and temporal trends in mean Hs between the four products during the recent satellite era (1992–2017). No attempt is made to examine how different products represent extreme sea states, as the issue of extremes in satellite altimeter and model data raises additional complexities that are beyond the scope of this short paper. Instead, we take advantage of the availability of the new CCI2019 altimeter product (ESA, 2019) to investigate for the first time wave height variability as represented by different altimeter products, prior to their wider uptake as reference datasets in climate research.

2. Sea State Datasets

The four sea state products used in this analysis (Table S1) form a diverse collection of high-quality datasets that are frequently used for wave climate validation and projections. This selection is not an implicit recommendation of these products and is not based upon any prior evaluation or statement of their accuracy.

2.1. Multimission Satellite Altimeter Products: RY2019 and CCI2019

The RY2019 dataset (Ribal & Young, 2019) is a level 2 product providing 32 years (1985 to 2017) of global altimeter measurements in a common standard form for 13 satellites including GEOSAT, ERS-1, TOPEX, ERS-2, GFO, JASON-1, ENVISAT, JASON-2, CRYOSAT-2, HY-2A, SARAL, JASON-3, and SENTINEL-3A. RY2019 gives access to unfiltered 1 Hz along-track measurements of Hs and wind speed for each individual altimeter mission. All data are subjected to calibration and validation against a selection of National Oceanographic Data Center (NODC) buoys. Careful quality control and calibration are applied to ensure long-term stability and cross-mission consistency. Results in this paper are based on gridded products (1° and 2°) generated for this study which exclude data from SARAL, JASON-3, and SENTINEL-3A.

The CCI2019 dataset corresponds to CCI Sea State version 1.1 level 4 product developed within the European Space Agency Climate Change Initiative for Sea State (Piollé, Dodet & Quilfen, et al., 2020). The CCI2019 dataset is a multimission-gridded (1°) product spanning 1992–2018. It extends the GlobWave dataset (1985–2016) up to 2018 by including more recent missions (JASON-3, SARAL, and CRYOSAT-2) but does not currently include GEOSAT nor SENTINEL-3A. CCI2019 is based on filtered 1 Hz along-track measurements of significant wave height, using empirical mode decomposition filtering (Huang et al., 1998) inspired from wavelet thresholding, as described in Kopsinis and McLaughlin (2009). The empirical mode decomposition filter significantly increases the signal-to-noise ratio at scales below 100 km (Quilfen & Chapron, 2019) which give clear benefits for the representation of Hs variability at the submesoscale but has limited impact on the large scales considered here.

During the GlobWave project (2008–2012), calibration methods were developed and applied to data from ERS-1, TOPEX, ERS-2, GFO, JASON-1, ENVISAT, and JASON-2 to account for changes in the Geophysical Data Records provided by space agencies. Most missions were linearly calibrated using match-ups with Hs measurements from an international network of buoys from the United States (National Data Buoy Center), Canada (Environment Canada), and Europe (Meteo-France, UK Met Office, and Spanish Puerto del Estado). One exception is TOPEX, for which data during the drifting period (1996–1999) were also corrected using crossovers with ERS-2 or GFO. Within CCI, more recent missions (JASON-3, SARAL, and CRYOSAT-2) and JASON-1 (for which GDR Version E products were recently released) were calibrated by correcting measurements globally against calibrated JASON-2 data. Details of the CCI calibration methodology and the calibration formulas for all missions can be found in the CCI Product User Guide V1.0 (Piollé, Dodet & Ash, et al., 2020) and associated past publications on this topic (Queffeulou, 2004; Queffeulou & Croizé-Fillon, 2009; Queffeulou et al., 2011).

2.2. Reanalysis and Hindcast Products: ERA5 and CY46R1

ERA5 (Hersbach et al., 2018) is the most recent release of the well-known and widely used reanalysis products developed and distributed by ECMWF. Replacing the previous successful ERA40 and ERA-Interim reanalyses, ERA5 provides a comprehensive high-resolution record of the global atmosphere, land surface, and ocean waves from 1950 onwards. ERA5 features a number of innovations, notably with hourly assimilation of altimeter significant wave height data. At the time of writing, ERA5 assimilates altimeter wave height data from most missions, except GEOSAT, TOPEX, SENTINEL-3A, and JASON-3. In this study, monthly mean Hs data at 0.5° horizontal resolution are used.

In addition, a more recent simulation with the ECMWF wave prediction system but run without assimilation has become available (ECMWF, 2019) to produce a long-term sea state hindcast. Even though waves in ERA5 already showed major improvements with respect to ERA-Interim, the CY46R1 wave hindcast are of even better quality than ERA5. The CY46R1 hindcast is a global wave model stand-alone run (i.e., not coupled), forced by ERA5 hourly 10-m neutral winds, surface air density, gustiness, and sea ice cover. Like ERA5, CY46R1 output is hourly, but CY46R1 has finer spatial and spectral resolutions (ERA5: 40 km, 24 directions, 30 frequencies; CY46R1: 14 km, 36 directions, 36 frequencies) and more recent global bathymetry (ERA5: ETOPO2; CY46R1: ETOPO1). CY46R1 also uses updated wave physics for wind input and dissipation. Importantly, in contrast to ERA5, no wave data assimilation is performed in CY46R1 (Bidlot et al., 2019). The absence of altimeter wave data assimilation in CY46R1 provides a higher degree of independence for the comparisons with satellite altimeter products. In this study, summaries of monthly Hs at 0.5° spatial resolution, that contributed to the recent updates to COWCLIP (Morim et al., 2019), are used.

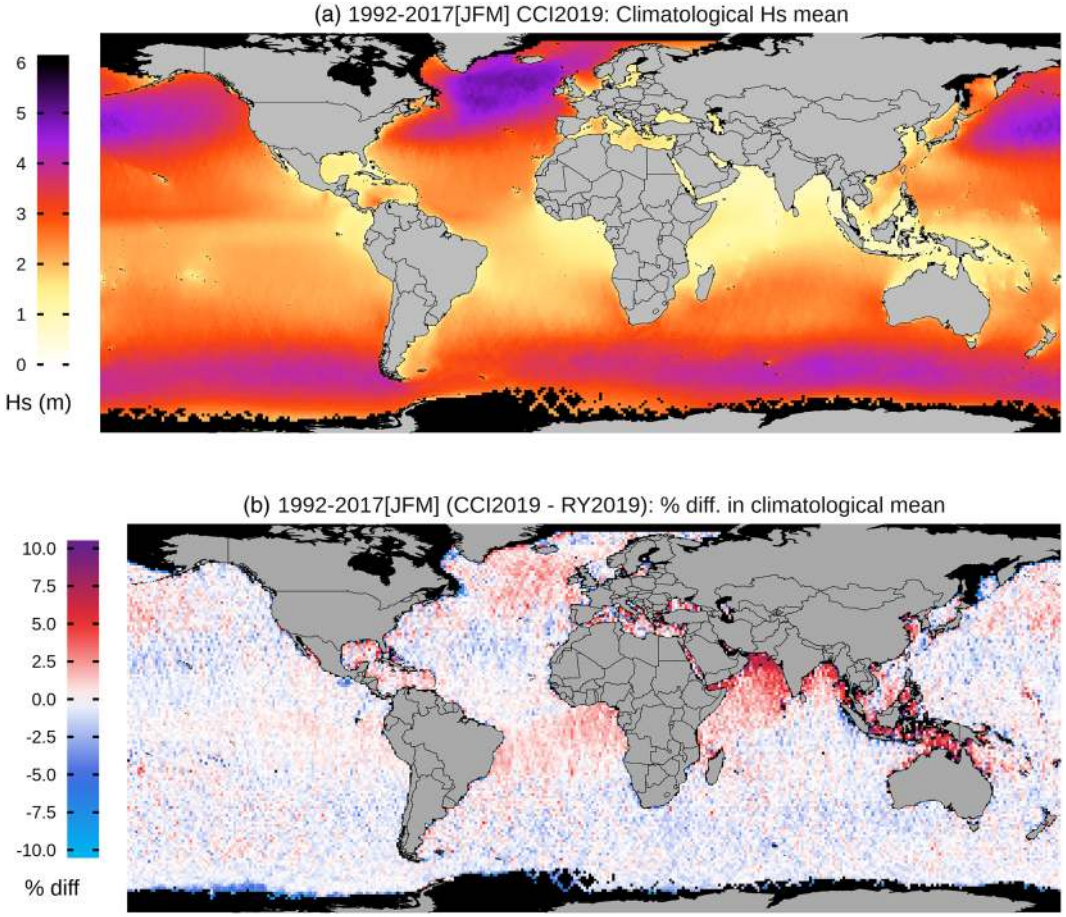

Figure 1. (a) Global climatological JFM mean Hs on a 1° × 1° grid computed over 1992–2017 for CCI2019 product. (b) Difference (%) between climatological mean Hs from CCI2019 and RY2019.

3. Analyses and Results

Differences between the various wave height products are examined first by comparing the global mean Hs climatology obtained with the two altimeter-based products, before considering temporal variability at two buoy locations, and global distributions of long-term trends in seasonal mean Hs. Important seasonal differences are accounted for by evaluating conditions separately for Northern Hemisphere winter (JFM) and summer (JAS); the latter is shown in the supporting information. Although reanalysis and hindcast data start in 1979, our interest in the altimeter products drives our evaluation of climatological mean and "long-term" trends to focus on the continuous satellite altimeter era, 1992 to 2017. Variation on longer time scales is examined in section 3.2.

3.1. Global Distributions of Climatological Mean Hs

Climatological mean Hs for the CCI2019 product is shown at its native 1° resolution in Figure 1a for JFM. Black pixels represent either values outside the color scale (above 10%, below −10%), or where minimum availability of 50% of the time series to compute a mean was not met. Energetic conditions in the NH, driven by extratropical storms, are clear in the midlatitudes. Smaller regional scale seasonal phenomena are also evident, such as waves in the eastern tropical Pacific driven by Tehuantepecer events at the Chivela Pass (Romero-Centeno et al., 2003). Contrast this with JAS (Figure S1a) that reveals corresponding energetic winter conditions in the Southern Ocean, along with other seasonal processes such as the Asian monsoon, manifesting in increased wave height in the Arabian Sea and Bay of Bengal.

Difference in the climatological average between the CCI2019 and RY2019 is shown in Figure 1b (JAS shown in Figure S1b). Across most of the ocean, relative differences are small (<2.5%), although in some locations reach 5%, with regions of positive and negative difference that exhibit spatial structure from the Equator

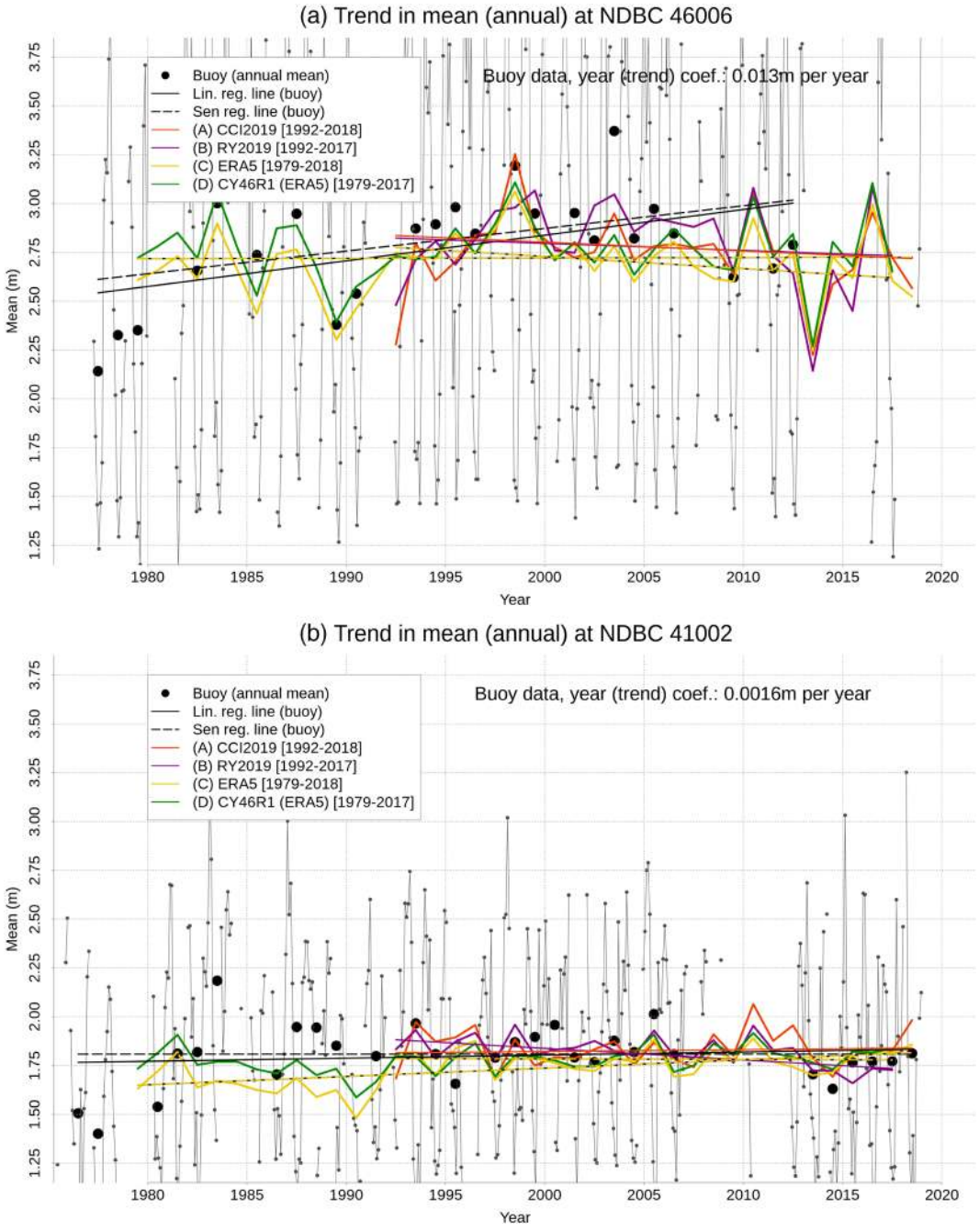

Figure 2. Time series of monthly and annual mean Hs (light and bold dots, respectively) from NDBC buoys 46006 (panel a) and 41002 (panel b) compared with annual mean Hs from four gridded products. Trends (solid colored lines) represent linear regressions of annual mean Hs. Dashed black line shows Sen regression of annual mean buoy Hs.

to midlatitudes. Enclosed and sheltered regions (Indonesia, Gulf of Mexico, Mozambique Channel, Arabian Sea, Red Sea, and Black Sea) in particular exhibit positive differences and, overall, correspond to regions of typically low sea state. Negative differences are spatially more diffuse, except for a slightly stronger patch corresponding approximately to the Asian monsoon in JAS (Figure S1b). Notwithstanding known caveats of applying significance testing to such sparse records, confidence estimates suggest that differences between the two products are generally not statistically significant, except in some low sea state regions (see Figure S2 and Text S3 for details).

3.2. Temporal Variability at Long-Term Buoy Locations

While our analyses focus on the period of continuous satellite coverage (1992 to 2017), it is informative to understand the context of sea state variability on longer timescales. For this, we chose to examine the sea state products at two locations with long-term in situ measurements from wave buoys. We therefore produce time series of monthly and annual mean Hs from buoy data and compare those with the gridded altimeter and simulation products. This also provides a means of examining the agreement between Hs from different products over time. Comparison with gridded products is performed by identifying the $1° \times 1°$ grid cell center that lies closest to the buoy location, with no further interpolation applied. Details of buoy data quality control and processing are given in Text S1.

Results are shown in Figure 2, first for NDBC buoy 46006 [Lat. 40.8N, Lon. 137.4W], deployed in 1977 in the eastern North Pacific (Figure 2a), which is a well-studied region with high variability and energetic conditions during NH winter; second, NDBC buoy 41002 [Lat. 31.9N, Lon. 74.9W], deployed in 1973 in the western North Atlantic (Figure 2b). The contrasting magnitude of the monthly Hs variability is clear, as is the difference of over 0.5-min climatological mean (not explicitly marked) for the complete period. Several prolonged periods of missing buoy data are observed at both sites, resulting in the loss of several annual Hs values. Over the period of analysis (1992 to 2017), agreement between the four products seems good, noting that the two satellite products are consistently higher than ERA5 and CY46R1, particularly at 46006 for RY2019 between 2000 and 2010.

Estimates of temporal trends in annual mean Hs are shown in Figure 2. Noting our focus on intercomparing data products rather than statistical methods, in this paper, trends are generally estimated using simple linear regression. More advanced methods, such as the Sen slope method and accompanying Mann-Kendall significance test (Sen, 1968; Hirsch et al., 1982), are often used to regress geophysical data, providing more robust estimates when data are non-normally distributed or affected by outliers. In Figure 2, trends for the buoy data (only) were estimated using both linear and Sen slope models, with similar results. Further results and discussion of regression methods is provided in Figure S3 and Text S2.

Focusing first on ERA5 and CY46R1, we note that the estimated linear trend is highly sensitive to the duration of the record. This is particularly clear at 46006, where dramatic trend sign changes occur between the satellite era and the longer period. Buoy data also suggest multidecadal variability on 20 years timescales, possibly linked at this site to the influence of the Pacific Decadal Oscillation. However, buoy 46006 is also one of few stations where the effects on Hs of periodic buoy configuration changes have been confirmed (Gemmrich et al., 2011), making it difficult to conclude about the differences observed with trends from ERA5 and CY46R1 over the full period. At 41002, although the trends are small, similar changes in trend signs over different periods occur. During the satellite era, trends at 41002 show excellent agreement between all products except RY2019 which alone reports negative trends. At 46006, the two altimeter products show similar (small negative) trends, which agree with trends in the simulation products (bar the 0.1 m offset already noted above).

3.3. Global Distributions of Trends in Mean Hs

Trends were estimated for all products for the period 1992–2017 at each grid cell over the full globe using linear regression (see also Text S2 and Figure S3 for further discussion of regression methods, including a comparison with the Sen slope method). Given the high variability of sea state in many regions, the spatial sampling density of altimeter data leads to large differences in signal-to-noise ratio in neighboring grid cells when gridding at 1° resolution. Trend maps at 1° resolution (not shown) reveal the altimeter sampling limitations with the appearance of "trackiness." Therefore, to better resolve the large scale spatial structure of trends, the RY2019 observations are aggregated here to 2° grid before estimating trends. For the other products that are all provided already on continuous uniform grids, similar aggregation to 2° is adopted, using the mean of the means of the constituent grid cells. Linear regression is then fitted independently at each $2° \times 2°$ grid cell location. The global maps of trends in mean Hs over 1992–2017 are shown for each product in Figure 3 for JFM (and in Figure S4 for JAS). Black dots indicate statistical significance of the trends in each product (see Text S3 for details).

Overall, the trends in seasonal mean Hs (JFM) over 1992–2017, over most of the globe, lie within $\pm$1cm/year for all products. However, in some regions (northern North Atlantic, north western Pacific, and Southern Ocean) a small number of grid cells exceed this, particularly for RY2019 and CCI2019, with the largest values tending to occur close to land and sea ice margins. The spatial structure of trends is coherent and shows some

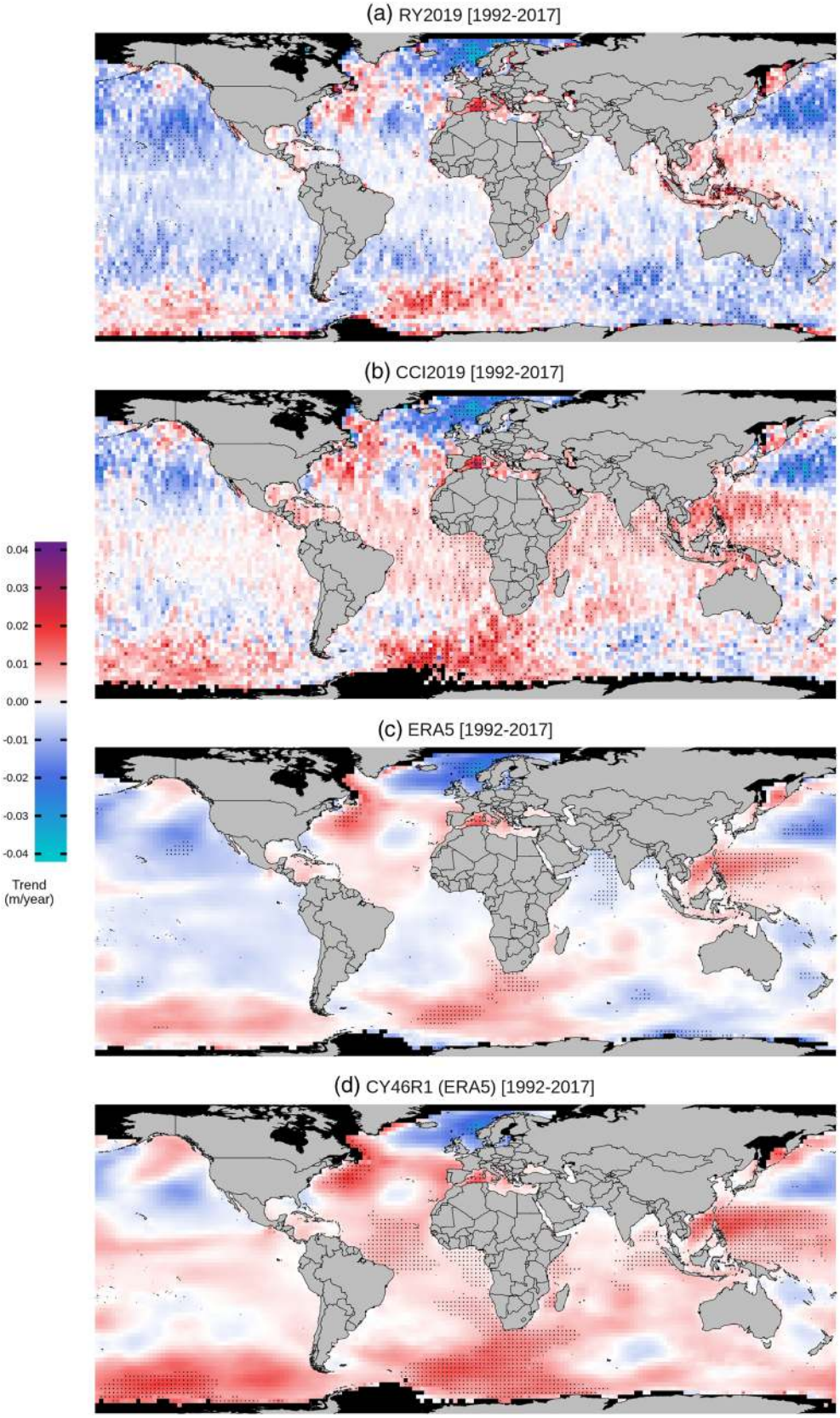

Figure 3. Global distribution of JFM mean Hs trend estimates on a 2° × 2° grid over 1992–2017 for (a) RY2019, (b) CCI2019, (c) ERA5, and (d) CY46R1. Dots indicate grid cells where the trend coefficient is significant at the 5% level.

similarity with patterns seen in Figure 1. Strong negative trends in the North Pacific, possibly associated with extratropical storm tracks, show up consistently across all products. Other regions of consistency include the Mediterranean and Norwegian seas. Strong positive trends in the Southern Ocean Atlantic sector (southwest of Africa) are also consistent. The spatially smooth trend structures in the simulation products (Figures 1c and 1d) contrast with the noisier patterns in the satellite products. Trends for JAS (Figure S4) reveal strong seasonal differences, including a large negative trend west of Australia that shows up consistently across all products.

The most striking aspect of this intercomparison remains, however, the differences in the magnitudes of the trends between products, observed for both JFM (Figure 3) and JAS (Figure S4), including a few locations where trends are statistically significant in different products. While the spatial structure appears remarkably consistency across products, qualitatively, the trend magnitude appears to increase steadily between products, from RY2019, showing the most negative trends, to CY46R1, showing the most positive. Strangely, the two altimeter products show some of the largest differences, even though they rely on broadly the same data. Even more strangely, perhaps the best agreement is obtained between CCI2019 and the CY46R1 hindcast, which does not assimilate altimeter data, although we note that during the development of CY46R1 some altimeter data (those received operationally) were used for validation of the tuning.

4. Discussion

4.1. Differences Between Altimeter-Based Sea State Products

The release of the CCI Sea State products, following closely after RY2019, provides a valuable means of reviewing the robustness of altimetry-based wave climate assessments obtained with independent processing of the same satellite source data. The preliminary analyses in this study appear to reveal important differences in climatologies and trends that raise immediate questions about uncertainty and the attribution of observed discrepancies to possible causes. The processing of these satellite observations is likely to be important, and it remains unclear whether, for example, the omission of SARAL mission data (2014 to 2016 inclusive) in our analysis of RY2019 has any impact.

The substantial climatological differences between the CCI2019 and RY2019 in low and high sea states noted in section 3.1 suggest biases affecting one or other (or both) products. A number of factors may explain these differences, both in terms of mean bias and trends. First, differences in mission data used (section 2.1) and subsequent impact on space-time sampling may impact estimates of monthly means. Further, the two products use different calibration methodologies and reference buoy data. RY2019 calibrate altimeter measurements against NDBC buoys around the United States, while CCI2019 first calibrates selected reference missions against U.S. NDBC buoys, Canadian (MEDS), and European (Meteo-France) networks, before intercalibrating the remaining missions against these reference missions (ESA, 2019; Queffeulou, 2004). Since the buoy network evolved significantly over 1992–2018 and some buoys are affected by changes in hull and payloads (Gemmrich et al., 2011), these differences could play an important role.

Moreover, RY2019 and CCI2019 use slightly different data editing criteria to remove spurious Hs measurements and different regression analysis to calibrate. Finally, RY2019 proposed a linear correction for CRYOSAT-2 while CCI2019 achieve better calibration using a nonlinear correction for this mission (ESA, 2019). Because CRYOSAT-2 data represent a significant fraction of the RY2019 data in our analyses, these differences may have a significant impact on estimated trends. The definition of the optimized calibration method for altimeter data is out of the scope of this study but clearly warrants further research to understand the uncertainties in altimeter wave climate studies related to calibration. In the meantime, it is clear that caution is advised against drawing firm conclusions about wave climate from these data, particularly in regions of discrepancy.

4.2. Differences in Trends

Quantifying long-term trends in sea state is an active area of research (Aarnes et al., 2015; Morim et al., 2019; Young et al., 2012; Young & Ribal, 2019). Most recently, Young and Ribal (2019) reported trends in Hs derived from the RY2019 data, which differ somewhat from our findings. Qualitatively, their trends (their Figure 2a) are generally within the same range globally, but they are markedly more positive than ours in some regions, including the Atlantic and Southern Ocean (Figure 3a). Direct quantitative comparison is not appropriate, however, given known differences in source data, postprocessing, and methodology. For example, Young and Ribal (2019) use all altimeter data from 1985 onwards (including GEOSAT), while our data start in 1992.

We partition the data into two seasonal averages (JFM and JAS) regressed with a linear model, as opposed to (Young & Ribal, 2019), who apply the seasonal Sen regression to each month concurrently to estimate a single trend.

The four trend maps in Figure 3 reveal striking differences also when applying the same estimation method to different products. Other factors thus contribute to the substantial variability in magnitude between products, such that the most accurate trend estimate is not at all clear. It is encouraging that all products show similar spatial distributions, with patterns recognizably associated with known ocean surface phenomena (e.g., tropics), although it remains unclear why trends should be more strongly positive in later products. Worthy of note is the surprisingly good agreement in trend magnitude and distributions between CCI2019 and CY46R1, all the more unexpected and promising for the hindcast's independence from altimeter data and use of advanced model physics.

Inspection of time series at buoy locations (Figures 2a and 2b) could not resolve the observed trend differences in different products nor help determine which product(s) best capture conditions at the buoys. The use of in situ observations remains problematic, as shown by the substantial quality control and data loss issues in Figure 2, notwithstanding the already mentioned problems with long-term buoy data consistency (Gemmrich et al., 2011). More dedicated efforts are urgently required to comprehensively understand and address these issues. The problem is compounded by the ubiquitous use of these sparse in situ observations for calibration and validation in the production of different types of data source (e.g., reanalysis, model, and satellite). The ensemble of products evaluated here could therefore reflect a complex mixture of much of the same information, and disentangling its dependence structure is extremely challenging.

A number of geophysical factors further complicate the evaluation of sea state trends driven by changing climate. Substantial temporal variability on interannual and decadal timescales is induced, for example, by strong regional modes of climatic variability, such as the North Atlantic oscillation. On the timescales of the records used here ($\sim$ 25 years), inconsistent or spurious representation of these strong modes in sea state products can bias estimated trends. For example, missing data within a time series could result in increased (or reduced) statistical weight being placed on observations in years that are strongly affected by a climatic mode, thus introducing bias. This raises methodological questions about the application of linear or non-parametric regression methods (Hirsch et al., 1982; Sen, 1968), which however versatile and robust with respect to identifying monotonic trends in univariate data (Alexander et al., 2006; Young & Ribal, 2019), cannot model the possible effects of additional covariates such as regional modes of variability over relevant timescales.

5. Conclusions

The recent release of the CCI2019 products presents a valuable opportunity to compare long-term changes in sea state in observational satellite records and highlighted the sensitivity of estimated trends to satellite data and methodological choices. Applying the same methodology to four high quality Sea State Climate Data records revealed important discrepancies, particularly in magnitude, and a tendency for later products to report larger positive trends globally. It appears that, despite increasing availability and duration of the observational records, many challenges still remain, among which is the question of what source can be regarded as the gold standard.

Our findings point to several areas for further research, notably about the reliability of buoy data for climate and the sensitivity of altimeter wave height to calibration. Detailed attribution of the differences in trends at the large scale and climatological differences at smaller scales (e.g., sheltered and coastal seas) would be desirable, as would robust determination of trends and uncertainties, once discrepancies between products are better understood. Finally, the important issue of extreme sea states, including at the coast, remains an important driver of future research. Young and Ribal (2019) suggest that stronger trends exist in more extreme sea states, so that differences in extremes between products are likely to be even more dramatic. Additional complexities specific to the estimation of extremes have to be considered, notably linked to altimeter space-time sampling of high sea states and calibration and quality control of extreme Hs values, and these form part of ongoing investigations within the ESA CCI Sea State project.

Acknowledgments
This work is part funded by the ESA Climate Change Initiative for Sea State project (AO/1-9041/17/I-NB). J-R Bidlot was supported by the WaveFlow project (CMEMS Service Evolution66-SE-CALL2). CCI Sea State data are available for download via http://cci.esa.int/data. Buoy data were obtained from the U.S. National Data Buoy Center (https://ndbc.noaa.gov).

References

Aarnes, O. J., Abdalla, S., Bidlot, J.-R., & Breivik, Ø. (2015). Marine wind and wave height trends at different ERA-Interim forecast ranges. *Journal of Climate*, *28*, 819–837. https://doi.org/10.1175/JCLI-D-14-00470.1

Alexander, L. V., Zhang, X., Peterson, T. C., Caesar, J., Gleason, B., Tank, A. M. G. K., et al. (2006). Global observed changes in daily climate extremes of temperature and precipitation. *Journal of Geophysical Research*, *111*, D05109. https://doi.org/10.1029/2005JD006290

Alves, J. H. G., & Young, I. R. (2003). On estimating extreme wave heights using combined Geosat, Topex / Poseidon and ERS-1 altimeter data. *Applied Ocean Research*, *25*, 167–186. https://doi.org/10.1016/j.apor.2004.01.002

Appendini, C. M., Torres-Freyermuth, A., Salles, P., López-Gonzólez, J., & Mendoza, E. T. (2014). Wave climate and trends for the Gulf of Mexico: A 30-yr wave hindcast. *Journal of Climate*, *27*, 1619–1632. https://doi.org/10.1175/JCLI-D-13-00206.1

Ardhuin, F., Stopa, J. E., Chapron, B., Collard, F., Husson, R., Jensen, R. E., et al. (2019). Observing sea states. *Frontiers*, *6*, 124. https://doi.org/10.3389/fmars.2019.00124

Ardhuin, F., Stutzmann, E., Schimmel, M., & Mangeney, A. (2011). Ocean wave sources of seismic noise. *Journal of Geophysical Research*, *116*, C09004. https://doi.org/10.1029/2011JC006952

Ash, E., Carter, D., & Collard, F. (2010). GlobWave satellite wave data quality report. D.16: Logica UK Ltd. http://globwave.ifremer.fr/download/GlobWave_D.16_SWDQR.pdf

Barnard, P. L., Hoover, D., Hubbard, D. M., Snyder, A., Ludka, B. C., Allan, J., et al. (2017). Extreme oceanographic forcing and coastal response due to the 2015-2016 El Niño. *Nature Communications*, *8*, 14365. https://doi.org/10.1038/ncomms14365

Bidlot, J.-R., Lemos, G., & Semedo, A. (2019). ERA5 reanalysis and ERA5-based ocean wave hindcast. http://www.waveworkshop.org/16thWaves/Presentations/R1%20Wave_Workshop_2019_Bidlot_et_al.pdf

Breivik, Ø., Aarnes, O. J., Abdalla, S., Bidlot, J.-R., & Janssen, P. A. E. M. (2014). Wind and wave extremes over the world oceans from very large ensembles. *Geophysical Research Letters*, *41*, 5122–5131. https://doi.org/10.1002/2014GL060997

Bricheno, L. M., & Wolf, J. (2018). Future wave conditions of Europe, in response to high-end climate change scenarios. *Journal of Geophysical Research: Oceans*, *123*, 8762–8791. https://doi.org/10.1029/2018JC013866

Bromirski, P. D., Flick, R. E., & Graham, N. (1999). Ocean wave height determined from inland seismometer data: Implications for investigating wave climate changes in the NE Pacific. *Journal of Geophysical Research*, *104*, 20,753–20,766.

Camus, P., Losada, I. J., Izaguirre, C., Espejo, A., Menéndez, M., & Pérez, J. (2017). Statistical wave climate projections for coastal impact assessments. *Earth's Future*, *5*, 918–933. https://doi.org/10.1002/2017EF000609

Cardone, V. J., Callahan, B. T., Chen, H., Cox, A. T., Morrone, M. A., & Swail, V. R. (2015). Global distribution and risk to shipping of very extreme sea states (vess). *International Journal of Climatology*, *35*, 69–84. https://doi.org/10.1002/joc.3963

Castelle, B., Dodet, G., Masselink, G., & Scott, T. (2018). Increased winter-mean wave height, variability and periodicity in the Northeast Atlantic over 1949–2017. *Geophysical Research Letters*, *45*, 3586–3596. https://doi.org/10.1002/2017GL076884

Collard, F., Ardhuin, F., & Chapron, B. (2005). Extraction of coastal ocean wave fields from SAR images. *IEEE Journal of Oceanic Engineering*, *30*, 526–533. https://doi.org/10.1109/JOE.2005.857503

Dodet, G., Bertin, X., & Taborda, R. (2010). Wave climate variability in the North-East Atlantic Ocean over the last six decades. *Ocean Modelling*, *31*, 120–131. https://doi.org/10.1016/j.ocemod.2009.10.010

ECMWF (2019). Official IFS Documentation CY46R1. In *chap. PART VII: ECMWF wave model*. Reading, UK: ECMWF. https://www.ecmwf.int/node/19311

ESA (2019). European Space Agency Climate Change Initiative for Sea State: Project website and data access. Retrieved 2019-07-10, from http://cci.esa.int/seastate

Gemmrich, J., Thomas, B., & Bouchard, R. (2011). Observational changes and trends in northeast Pacific wave records. *Geophysical Research Letters*, *38*, L22601. https://doi.org/10.1029/2011GL049518

Gommenginger, C. P., Srokosz, M. A., Challenor, P. G., & Cotton, P. D. (2002). Development and validation of altimeter wind speed algorithms using an extended collocated buoy/TOPEX data set. *IEEE Transactions on Geoscience and Remote Sensing*, *40*, 251–260. https://doi.org/10.1109/36.992782

Hell, M. C., Cornelle, B. D., Gille, S. T., Miller, A. J., & Bromirski, P. D. (2019). Identifying ocean swell generation events from Ross ice shelf seismic data. *Journal of Atmospheric and Oceanic Technology*, *36*, 2171–2189. https://doi.org/10.1175/JTECH-D-19-0093.1

Hersbach, H., de Rosnay, P., Bell, B., Schepers, D., Simmons, A., Soci, C., et al. (2018). Operational global reanalysis: Progress, future directions and synergies with NWP (Tech. Rep.). European Centre for Medium Range Weatherforecasting. https://www.ecmwf.int/en/elibrary/18765-operational-global-reanalysis-progress-future-directions-and-synergies-nwp

Hirsch, R. M., Slack, J. R., & Smith, R. A. (1982). Techniques of trend analysis for monthly water quality data. *Water Resources Research*, *18*, 107–121. https://doi.org/10.1029/WR018i001p00107

Huang, N. E., Shen, Z., Long, S. R., Wu, M. C., Shih, H. H., Zheng, Q., et al. (1998). The empirical mode decomposition and the Hilbert spectrum for nonlinear and non-stationary time series analysis. *Proceedings of the Royal Society of London A: Mathematical, Physical and Engineering Sciences*, *454*, 903–995. https://doi.org/10.1098/rspa.1998.0193

Izaguirre, C., Méndez, F. J., Menéndez, M., & Losada, I. J. (2011). Global extreme wave height variability based on satellite data. *Geophysical Research Letters*, *38*, L10607. https://doi.org/10.1029/2011GL047302

JCOMM DBCP (2019). Data Buoy Cooperation Panel. Retrieved 2019-12-27, https://www.jcomm.info/index.php?option=com_content&view=article&id=65:wave-measurement-evaluation-and-test-3&catid=18&Itemid=2

Kopsinis, Y., & McLaughlin, S. (2009). Development of EMD-based denoising methods inspired by wavelet thresholding. *IEEE Transactions on Signal Processing*, *57*, 1351–1362. https://doi.org/10.1109/TSP.2009.2013885

Lehner, S., Schulz-Stellenfleth, J., SchÃđttler, B., Breit, H., & Horstmann, J. (2000). Wind and wave measurements using complex ERS-2 SAR wave mode data. *IEEE Transactions on Geoscience and Remote Sensing*, *38*, 2246–2257.

Massom, R. A., Scambos, T. A., Bennetts, L. G., Reid, P., Squire, V. A., & Stammerjohn, S. E. (2018). Antarctic ice shelf disintegration triggered by sea ice loss and ocean swell. *Nature*, *558*, 383–389. https://doi.org/10.1038/s41586-018-0212-1

Morim, J., Hemer, M., Cartwright, N., Strauss, D., & Andutta, F. (2018). On the concordance of 21st century wind-wave climate projections. *Global and Planetary Change*, *167*, 160–171. https://doi.org/10.1016/j.gloplacha.2018.05.005

Morim, J., Hemer, M., Wang, X. L., Cartwright, N., Trenham, C., Semedo, A., et al. (2019). Robustness and uncertainties in global multivariate wind-wave climate projections. *Nature Climate Change*, *9*, 711–718. https://doi.org/10.1038/s41558-019-0542-5

Piollé, J.-F., Dodet, G., & Ash, E. (2020). ESA Sea State Climate Change Initiative: Product user guide, version 1.0. http://dap.ceda.ac.uk/thredds/fileServer/neodc/esacci/sea_state/docs/v1.1/Sea_State_cci_PUG_v1.0-signed.pdf

Piollé, J.-F., Dodet, G., & Quilfen, Y. (2020). ESA Sea State Climate Change Initiative : Global remote sensing merged multi-mission monthly gridded significant wave height, L4 product, version 1.1., Centre for Environmental Data Analysis, European Space Agency, CCI for Sea State Consortium. http://doi.org/10.5285/47140d618dcc40309e1edbca7e773478

Queffeulou, P. (2004). Long-term validation of wave height measurements from altimeters. *Marine Geodesy*, *27*, 495–510. https://doi.org/10.1080/01490410490883478

Queffeulou, P., Ardhuin, F., & Lefèvre, J.-M. (2011). Wave height measurements from altimeters: Validation status and applications. https://www.aviso.altimetry.fr/fileadmin/documents/OSTST/2011/poster/Queffeulou_posterOSTST.pdf

Queffeulou, P., & Croizé-Fillon, D. (2009). La mesure satellite de hauteur de vague par altimÃĺtre: Tat des lieux, application la climatologie et la mod-lisation des tats de mer, *Les ateliers de modlisation de atmosphre*. Toulouse. ftp://ftp.ifremer.fr/ifremer/cersat/products/swath/altimeters/waves/documentation/publications/ama_2009_queffeulou_croize-fillon.pdf

Quilfen, Y., & Chapron, B. (2019). Ocean surface wave-current signatures from satellite altimeter measurements. *Geophysical Research Letters*, *46*, 253–261. https://doi.org/10.1029/2018GL081029

Ribal, A., & Young, I. R. (2019). 33 years of globally calibrated wave height and wind speed data based on altimeter observations. *Scientific data*, *6*, 1–15. https://doi.org/10.1038/s41597-019-0083-9

Romero-Centeno, R., Zavala-Hidalgo, J., Gallegos, A., & O'Brien, J. J. (2003). Isthmus of Tehuantepec wind climatology and ENSO signal. *Journal of Climate*, *16*, 2628–2639.

Semedo, A., SuÅąelj, K., Rutgersson, A., & Sterl, A. (2011). A global view on the wind sea and swell climate and variability from ERA-40. *Journal of Climate*, *24*, 1461–1479. https://doi.org/10.1175/2010JCLI3718.1

Sen, P. K. (1968). Estimates of the regression coefficient based on Kendall's Tau. *Journal of the American Statistical Association*, *63*, 1379–1389. https://doi.org/10.1080/01621459.1968.10480934

Shimura, T., Mori, N., & Mase, H. (2015). Future projections of extreme ocean wave climates and the relation to tropical cyclones: Ensemble experiments of MRI-AGCM3.2H. *Journal of Climate*, *28*, 9838–9856.

Stopa, J. E., Cheung, K. F., Tolman, H. L., & Chawla, A. (2013). Patterns and cycles in the climate forecast system reanalysis wind and wave data. *Ocean Modelling*, *70*, 207–220. https://doi.org/10.1016/j.ocemod.2012.10.005

Storlazzi, C. D., Gingerich, S. B., van Dongeren, A., Cheriton, O. M., Swarzenski, P. W., Quataert, E., et al. (2018). Most atolls will be uninhabitable by the mid-21st century because of sea-level rise exacerbating wave-driven flooding. *Science Advances*, *4*, eaap9741. https://doi.org/10.1126/sciadv.aap9741

Swail, V., Jensen, R. E., Lee, B., Turton, J., Thomas, J., Gulev, S., et al. (2009). Wave measurements, needs and developments for the next decade. In *Proceedings of OceanObs'09, Sustained Ocean Observations and Information for Society, Venice, Italy, 21-25 September 2009 (ESA, publication wpp-306).* https://doi.org/10.5270/OceanObs09

Thomas, S., Babanin, A. V., Walsh, Kevin, J. E., Stoney, L., & Heil, P. (2019). Effect of wave-induced mixing on Antarctic sea ice in a high-resolution ocean model. *Ocean Dynamics*, *69*, 737–746. https://doi.org/10.1007/s10236-019-01268-0

Woolf, D. K., Challenor, P. G., & Cotton, P. D. (2002). Variability and predictability of the North Atlantic wave climate. *Journal of Geophysical Research*, *107*, 3145. https://doi.org/10.1029/2001JC001124

Young, I. R., & Ribal, A. (2019). Multiplatform evaluation of global trends in wind speed and wave height. *Science*, *364*, 548–552. https://doi.org/10.1126/science.aav9527

Young, I. R., Vinoth, J., Zieger, S., & Babanin, A. V. (2012). Investigation of trends in extreme value wave height and wind speed. *Journal of Geophysical Research*, *117*, C00J06. https://doi.org/10.1029/2011JC007753

Zieger, S., Vinoth, J., & Young, I. R. (2009). Joint calibration of multiplatform altimeter measurements of wind speed and wave height over the past 20 years. *Journal of Atmospheric and Oceanic Technology*, *26*, 2549–2564. https://doi.org/10.1175/2009JTECHA1303.1